

Scattering of Negative Pions by Hydrogen*

E. FERMI, M. GLICKSMAN, R. MARTIN, and D. NAGLE†
Institute for Nuclear Studies, University of Chicago, Chicago, Illinois
 (Received June 24, 1953)

The scattering of negative pions by liquid hydrogen has been studied with the 450-Mev synchrocyclotron, using the pion beams of energy 169 Mev, 194 Mev, and 210 Mev. Angular distributions for ordinary scattering and for photon production are presented for each of the three primary energies. The differential cross sections for ordinary scattering and for charge-exchange scattering are computed for the center-of-mass system. The charge-exchange cross sections when plotted as a function of the energy appear to go through a maximum at about 180 Mev. On the other hand, the ordinary scattering cross sections appear to increase steadily with the energy. The charge exchange cross sections, which at lower energies are predominantly backward, become rapidly forward as the energy increases, and are strongly forward at the highest energy.

THE scattering of negative pions by hydrogen has been investigated in this laboratory using the pion beams of the 450-Mev synchrocyclotron. In the present paper, the results of previous measurements¹ are extended to a higher energy range. With our present technique this is possible only for negative pions because the intensity of the external positive pion beams from the cyclotron becomes extremely small at high energy. In the work here reported, the elastic and the charge-exchange scattering of negative pions on hydrogen have been investigated for primary pion beams of 169 Mev, 194 Mev, and 210 Mev. The equipment and the experimental technique used in this measurement are essentially the same as those already described in A. A beam of pions of the desired energy passes through two scintillation counters No. 1 and No. 2 and after that traverses a thin-walled liquid hydrogen Dewar. The scattered particles are detected by two other counters No. 3 and No. 4. The double coincidences of No. 1 and No. 2, indicated by D , give a measure of the number of primary particles. The quadruple coincidences of the four counters, indicated by Q , give a measure of the number of scattered particles that are detected by the detecting counters No. 3 and No. 4. For an average rate of cyclotron operation corresponding to 20 watts on the target, the double coincidences per minute were approximately 190 000 at 169 Mev, 53 000 at 194 Mev, and 35 000 at 210 Mev.

For the details and geometry of this arrangement, we refer to Sec. I of A. One difference in the present experiments was in the construction of counters No. 1 and No. 2, which had the same diameter of 2 in. as in A, but were much thinner. Counter No. 1 in these experiments was a liquid scintillator with an over-all thickness of $\frac{1}{4}$ in., and counter No. 2 was a plastic scintillator $\frac{1}{8}$ in. thick. The background due to star production from the collisions with counter No. 2 is thereby reduced very considerably. In the previous experiments the thickness of the detecting counters

was sufficient to prevent the detection of the recoil protons even for the measurements at 45° scattering angle. In the present measurements at higher energies, it was necessary in some cases to insert some additional absorber in front of counter No. 4 in order to make sure that no recoil protons could be detected. Such additional absorbers were used only in the measurements at 194 Mev and 210 Mev and only for scattering angle of 45° . In the measurements at 194 Mev an extra absorber of $\frac{5}{8}$ -in. aluminum was inserted in the runs without lead radiator. In the measurements at 210 Mev, an extra absorber of $\frac{1}{8}$ -in. aluminum was used when the lead radiator was in place; without lead radiator, the extra absorber was $\frac{7}{8}$ -in. aluminum. Otherwise the procedure followed in the calculation and reduction of the data is identical to the one described in Sec. VII of A.

Scattering measurements are taken for the laboratory scattering angles 45° , 90° , and 135° and at each position four measurements of the ratio Q/D between quadruple and double coincidences are taken with and without liquid hydrogen in the Dewar and with and without a lead plate of 7.36 g/cm² placed in front of counter No. 3. The difference of the measurements with and without liquid hydrogen is taken as the effect due to the presence of the liquid hydrogen. The lead plate increases the sensitivity of the detecting counters to the photons produced in the decay of the neutral pions in the charge exchange process. Table I summarizes the observed values of the ratio Q/D obtained in the present measurements. This table is the analog of Table VI of A.

In order to compute from the data of this table the numbers of scattered pions and photons entering the detecting counters No. 3 and No. 4, one needs the efficiencies with and without lead radiator for the two types of particles. The procedure for calculating these efficiencies is described in Sec. 8 of A. The only difference is the extra absorption due to the aluminum absorbers which were put in some of the measurements in front of counter No. 4 in order to stop all the recoil protons. The efficiencies adopted in the calculation are summarized in Table II.

* Research supported by a joint program of the U. S. Office of Naval Research and the U. S. Atomic Energy Commission.

† Aided by a grant from the Guggenheim Foundation.

¹ Anderson, Fermi, Martin, and Nagle, Phys. Rev. **91**, 155 (1953), quoted here as A.

TABLE I. Observed values of $(Q/D) \times 10^6$ for negative pions.

169 Mev (94% pions)				
Angle	Lead	With hydrogen	Without hydrogen	Net
45°	out	269.4± 7.9	141.7±5.1	127.7± 9.4
90°	out	100.8± 4.3	60.5±3.6	40.3± 5.7
135°	out	160.9± 5.4	83.2±4.1	77.7± 6.8
45°	in	488.8±11.1	121.5±5.1	367.3±12.1
90°	in	243.4± 6.7	58.8±3.5	184.6± 7.6
135°	in	303.8± 7.4	77.4±4.0	226.4± 8.4
194 Mev (96% pions)				
45°	out	295±11	137±8	158±14
90°	out	112± 6	53±4	59± 7
135°	out	176± 8	91±5	85± 9
45°	in	638±15	169±9	469±18
90°	in	278±10	63±6	215±12
135°	in	344± 6	92±6	252± 8
210 Mev (98% pions)				
45°	out	288±14	121±8	167±16
90°	out	146± 9	72±6	74±11
135°	out	171±11	89±7	82±13
45°	in	633±20	155±9	478±22
90°	in	222±12	63±6	159±14
135°	in	263±13	93±7	170±15

For each primary energy and each scattering angle, one computes with these efficiencies, from the data of Table I, the numbers Π and Γ of pions and photons entering the solid angle subtended by counter No. 4. This is done by solving two equations with two unknowns as described in A.

The numbers Π and Γ can immediately be converted to cross sections per steradian for the two processes. In order to do this, they must be divided by the product of the following factors: (a) the number of pions per million doubles. This number was obtained as in A, from a study of the absorption curve. The percentage of pions in the beam of the various energies is given in Table I. (b) The solid angle subtended by counter No. 4. This was as in A, 0.083 steradians. (c) The number of

TABLE II. Efficiencies of the detecting counters.

Energy (Mev)	Angle	Lead	Efficiency for pions (percent)	Efficiency for photons (percent)
169	45°	out	97	4
	45°	in	92	71
	90°	out	97	4
	90°	in	90	64
	135°	out	97	4
194	135°	in	89	61
	45°	out	92	4
	45°	in	92	72
	90°	out	97	4
	90°	in	91	66
210	135°	out	97	4
	135°	in	90	62
	45°	out	90	4
	45°	in	91	73
	90°	out	97	4
90°	in	91	67	
135°	out	97	4	
135°	in	91	63	

TABLE III. Differential cross sections for negative pions

Energy (Mev)	Process	Laboratory system		Center-of-mass system	
		Scattering angle (degrees)	Diff. cross section ($10^{-27}\text{cm}^2/\text{sterad}$)	Scattering angle (degrees)	Diff. cross section ($10^{-27}\text{cm}^2/\text{sterad}$)
169	$\pi^- \rightarrow \pi^-$	45	2.56±0.35	56.6	1.82±0.25
		90	0.69±0.16	105.4	0.73±0.17
169	$\pi^- \rightarrow \gamma$	135	1.51±0.22	145.2	2.31±0.34
		45	8.05±0.94	54.9	6.05±0.71
194	$\pi^- \rightarrow \pi^-$	90	5.37±0.63	102.8	5.65±0.66
		135	5.95±0.72	143.4	8.37±1.01
194	$\pi^- \rightarrow \gamma$	45	3.28±0.50	57.3	2.30±0.35
		90	1.08±0.20	106.0	1.16±0.21
210	$\pi^- \rightarrow \pi^-$	135	1.62±0.27	145.6	2.54±0.42
		45	9.87±1.23	55.6	7.24±0.90
210	$\pi^- \rightarrow \gamma$	90	5.53±0.74	103.7	5.87±0.79
		135	6.41±0.77	143.9	9.29±1.12
210	$\pi^- \rightarrow \pi^-$	45	3.49±0.53	57.9	2.43±0.37
		90	1.47±0.29	106.7	1.59±0.31
210	$\pi^- \rightarrow \gamma$	135	1.64±0.36	146.0	2.61±0.57
		45	9.43±1.27	56.1	6.83±0.92
210	$\pi^- \rightarrow \gamma$	90	2.99±0.66	104.4	3.19±0.70
		135	3.31±0.77	144.4	4.88±1.14

hydrogen atoms per cm^2 traversed by the beam. As in A, this number was 5.9×10^{23} . (d) A correction factor due to the attenuation of the primary beam while traversing the hydrogen cell. For the three energies these correction factors were estimated to be 0.988, 0.986, and 0.990.

The differential cross sections so obtained and their conversions to the center-of-mass system are collected in Table III. The errors listed in this table are compounded out of the statistical error plus a 10 percent error that we estimate may be due to our imperfect knowledge of the sensitivity of the detecting equipment.

From the differential cross sections in the laboratory system one obtains immediately by integration the total cross sections listed in Table IV. In columns 2 and 3 are given the total cross sections for elastic scattering and for the photon producing process. The contribution of this last process to the total cross section is only half the cross section listed in column 3, because each disintegrating neutral pion yields two photons. For this reason, the total cross sections given in column 4 are obtained by adding half the cross section for photon production to the elastic scattering cross section. A small amount of approximately 0.5 mb has been added in order to take into account the contribution of the inverse photoeffect. In the last column the values of the total cross section from transmission

TABLE IV. Integrated cross sections of negative pions (10^{-27}cm^2).

Energy (Mev)	$\pi^- \rightarrow \pi^-$	$\pi^- \rightarrow \gamma$	Total	Total from transmission
169	21.2±2.0	82.8±5.9	63±4	64±6
194	26.4±2.7	93.9±7.2	74±5	66±6
210	28.7±3.1	69.1±7.2	64±5	61±6

experiments are listed for comparison. They are obtained by interpolation from data already published.²

On the assumption that only s and p levels contribute to the interaction, one expects that all the cross sections in the center-of-mass system should be of the form

$$a + b \cos\vartheta + c \cos^2\vartheta. \quad (1)$$

The assumption that the contribution of d scattering is negligible becomes, of course, less and less plausible as the energy increases and it is very questionable whether it is correct for pions of approximately 200 Mev. A check on this assumption and formula (1) that derives from it would require a more thorough study of the angular dependence of the scattering than has been possible until now. Assuming formula (1) to be correct, one can compute from the data of Table III the values of the coefficients a , b , and c that represent the experimental data. These values are collected in Table V.

CONCLUSIONS

In Fig. 1 we have plotted the observed differential cross sections in the laboratory system listed in Table

TABLE V. Coefficients of $d\sigma/d\omega = a + b \cos\vartheta + c \cos^2\vartheta$ for various processes ($10^{-27}\text{cm}^2/\text{sterad}$).

Energy (Mev)	λ (10^{-10}cm)	Process	a	b	c
169	0.928	$\pi^- \rightarrow \pi^-$	0.64 ± 0.19	0.47 ± 0.29	3.04 ± 0.62
		$\pi^- \rightarrow \gamma$	5.28 ± 0.69	-0.84 ± 0.86	3.76 ± 2.00
		$\pi^- \rightarrow 0$	1.85 ± 0.72	-0.61 ± 0.62	4.25 ± 2.27
194	0.856	$\pi^- \rightarrow \pi^-$	1.12 ± 0.24	0.65 ± 0.40	2.87 ± 0.80
		$\pi^- \rightarrow \gamma$	5.53 ± 0.83	-0.13 ± 1.06	5.59 ± 2.48
		$\pi^- \rightarrow 0$	1.73 ± 0.80	-0.09 ± 0.74	5.89 ± 2.61
210	0.817	$\pi^- \rightarrow \pi^-$	1.56 ± 0.34	0.50 ± 0.47	2.14 ± 1.09
		$\pi^- \rightarrow \gamma$	3.55 ± 0.75	2.82 ± 1.06	5.48 ± 2.28
		$\pi^- \rightarrow 0$	0.84 ± 0.70	1.94 ± 0.73	5.56 ± 2.31

III versus the energy of the primary pions. For comparison also the cross sections obtained in A at the energies of 120 and 144 Mev have been included. Examination of this figure shows a rather striking difference in behavior of the cross sections for the elastic scattering and for the photon producing process. The former cross sections increase steadily with energy without any apparent sharp feature. On the other hand, the cross sections for photon production appear to go through a maximum at approximately 180 Mev. A second feature of these cross sections is the very rapid increase of the forward cross section with respect

² Anderson, Fermi, Long, Martin, and Nagle, Phys. Rev. **85**, 934 (1952).

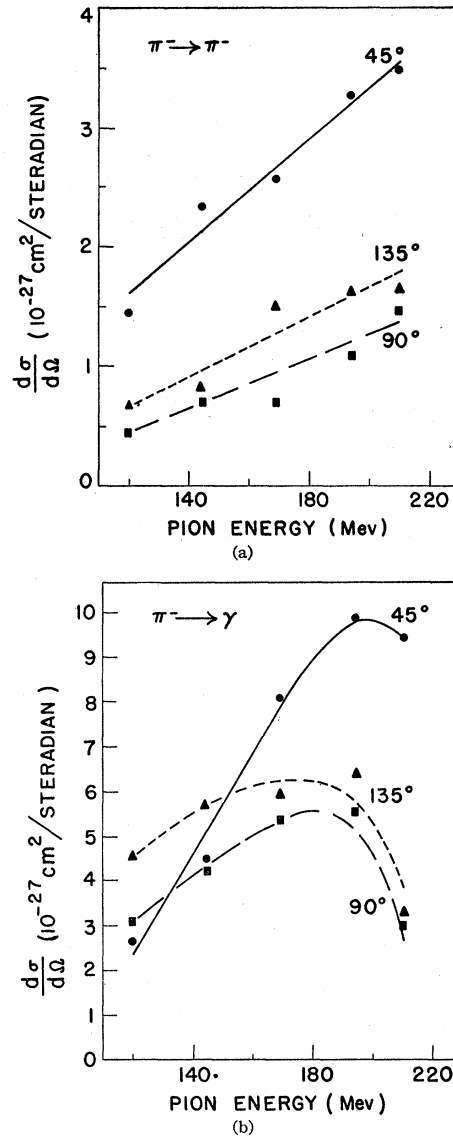


FIG. 1. Differential cross sections in the laboratory system for negative pions on hydrogen as functions of the primary pion energy. (a) Elastic scattering. The three curves correspond to laboratory scattering angles 45° , 90° , and 135° . The curves are graphical interpolations of the data. (b) Cross sections for photon production at the same angles.

to the others. Due to this increase, the scattering which is mostly backward at the low energies becomes mostly forward at the high energies. This feature is recognizable also from the data of Table V which show a change in sign from negative to positive in the coefficient b for the exchange scattering.